UC Berkeley
UC Berkeley Previously Published Works

Title

Effects of laser-induced heating on nitrogen-vacancy centers and single-nitrogen defects in diamond

Permalink

Journal

ISSN

Authors

Szczuka, Conrad
Drake, Melanie
Reimer, Jeffrey A

Publication Date

DOI

Peer reviewed

Effects of laser-induced heating on nitrogen-vacancy centers and single-nitrogen defects in diamond

Conrad Szczuka[1], Melanie Drake[2] and Jeffrey A Reimer[2]

[1] Department of Chemistry, RWTH Aachen University, 52062 Aachen, Germany
[2] Department of Chemical and Biomolecular Engineering, University of California, Berkeley, CA 94720, United States of America

E-mail: conrad.szczuka@rwth-aachen.de

CrossMark

Abstract

We investigate the effects of laser-induced heating of NV^- and P1 defects in diamonds by X-band CW EPR spectroscopy, with particular attention to temperature effects on the zero field splitting and electron polarization. A 532 nm laser with intensities of 7–36 mW mm^{-2} is sufficient to heat diamond samples from room temperature to 313–372 K in our experimental setup. The temperature effects on the determined NV^- zero-field splittings are consistent with previously observed non-optical heating experiments. Electron spin polarization of the NV^- defects were observed to increase, then saturate, with increasing laser light intensities up to 36 mW mm^{-2} after accounting for heating effects. We observe that EPR signal intensities from P1 centers do not follow a Boltzmann trend with laser-induced sample heating. These findings have bearing on the design of diamond-based polarization devices and magnetometry applications.

Keywords: diamond, nitrogen vacancy, substitutional nitrogen, EPR, laser-induced heating, temperature, hyperpolarization

S Supplementary material for this article is available online

(Some figures may appear in colour only in the online journal)

1. Introduction

Negatively charged nitrogen-vacancy centers (NV^-) in diamonds are C_{3v}-symmetry defects and consist of a substitutional nitrogen and an adjacent carbon-vacancy [1]. Upon optical excitation, spin-dependent intersystem crossing rates in the excited triplet state result in spin polarization into the zero spin state [2, 3]. A zero-field magnetoanisotropic effect splits the ground state electron Zeeman magnetic sublevels $m_s = 0$ and $m_s = \pm 1$ by $D_{\text{ref}} \approx 2.87$ GHz [4].

The NV^- center is greatly promising for various quantum technologies and has already been examined for applications including thermometry [5, 6], magnetometry [7, 8], electrometry [9, 10], as a single photon source [11] and as a nano-biosensor [12]. The easily accessible electron Zeeman hyperpolarization offers utilization in magnetic spectroscopy and imaging through strongly enhanced resolution; also through transfer of polarization to neighboring nuclear and electron spins [13–22]. These applications require accurate knowledge of the zero field splitting and/or the degree of NV^- polarization.

The effects of pressure [23, 24], electric fields [25], and temperature [26–30] on the zero field splitting of NV^- were studied recently, as well as the effect of changing temperature on photoluminescence [5]. These parameters were adjusted by

an additional experimentally controlled device, such as applied electric fields. In contrast, we evaluate herein the temperature effects caused by the use of a hyperpolarizing laser. High laser intensities cause significant enough heating to see temperature dependent changes in NV$^-$ zero-field splitting [26, 28–30] and a substantial reduction of hyperpolarization and saturation behavior at laser intensities of 8–25 mW mm^{-2} [25, 31, 32].

We report time-dependent laser-induced heating effects on NV$^-$ and substitutional nitrogen (P1) defects in HPHT Ib diamonds by X-band CW EPR spectroscopy. After accounting for laser heating effects, we find that NV$^-$ electron polarization decreases with increasing temperature as expected, and increases with laser illumination intensity at isothermal conditions. EPR signal intensities associated with P1 centers also decrease with temperature, independent of laser intensity. Strikingly, the observed decreases are not consistent with estimates based upon a Boltzmann distribution of populations for the P1 magnetic sublevels.

2. Materials and methods

The six diamonds used in this study are $2 \times 2 \times 0.3$ mm HPHT type Ib diamonds purchased from Sumitomo, Inc. They were treated with 1 MeV electron irradiation (Prism Gem) and subsequently annealed at 800 °C for 2 h under 9%H$_2$/91%He gas flow. These diamonds are samples #3–#8 in a previously published study [33]. Defect concentrations of NV$^-$ (4.2–8.7 ppm) and P1 (22–101 ppm) were determined [33] using X-band EPR. We retain the same sample numbering here for convenience.

X-band CW EPR experiments were performed in a modified active spectrum$^{\copyright}$ extended range benchtop EPR system. Optical access to the sample was added perpendicular to the magnetic field direction by mounting a 45° mirror underneath a hole in the bottom of the microwave cavity. Samples were mounted with varnish on the end of a fiberglass rod. The microwave power incident on the cavity was set to 0.158 μW for NV$^-$ and 1.58 μW for P1 center analysis. If not stated differently, spectra were recorded with 1 scan, 100 data points per mT using a conversion time of 100 ms, a modulation frequency of 43 kHz, and amplitude of 0.2 mT. Optical pumping was realized by sample illumination with 532 nm circularly polarized laser light with a beam diameter of 5 mm. NV defect concentrations in our samples absorb ≈73% of 532 nm laser light. (see reference 1 in supplemental material (stacks.iop.org/JPhysD/50/395307/mmedia)). Applied laser intensities range from 0.5–36 mW mm^{-2}. NV$^-$ polarization was measured through peak-to-peak intensity of the acquired dispersive EPR spectrum.

For *in situ* recording of laser-induced temperature rise, a thermocouple was inserted into the microwave cavity alongside the fiberglass rod and fixed on the surface of the diamond with varnish. Time-dependent temperature calibration (see 3, supplemental material) was performed without microwaves applied over the range of 0–120 s of laser exposure. Regrettably, EPR spectra could not be acquired with a thermocouple inside the microwave cavity.

Laser-independent heating measurements on P1 centers were performed by placing the diamond in a liquid sample
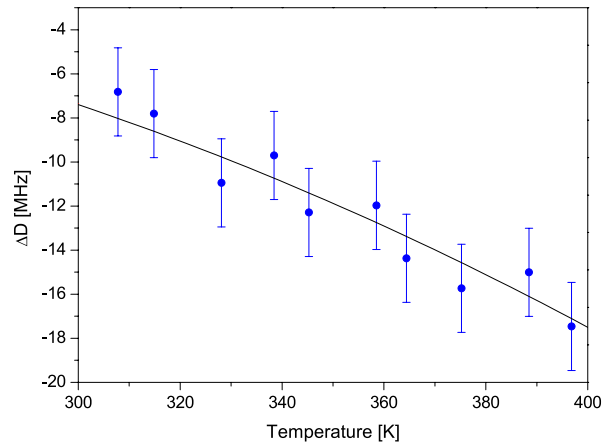

Figure 1. Difference ΔD between the measured axial zero-field splitting parameter and its reference value (2.87 GHz) with increasing temperature for sample #8. The NV$^-$ $|0\rangle \rightarrow |+1\rangle$ spin state transitions were analyzed to yield the zero-field splitting. The black line represents results from the literature [30] and the blue dots the present EPR data.

EPR tube filled 4 cm high with heated silicon oil. EPR measurements were subsequently acquired after calibrated waiting times to achieve specified sample temperatures. Calibrations were performed using a thermocouple inside the EPR tube without applying microwaves.

3. Results and discussions

3.1. Laser-induced temperature effects on NV$^-$ zero field splitting

Figure 1 shows the decrease of the NV$^-$ axial zero-field splitting parameter D with temperature. The temperature change was the result of illumination with 532 nm circularly polarized laser light having intensities varying from 2–48 mW mm^{-2} and exposure times of 120 s. For NV$^-$ transitions from $|0\rangle$ to $|+1\rangle$, ΔD was calculated using

$$\Delta D = D_{obs}(T, \theta) - D_{ref} = \left(\nu_{mw} - \frac{\mu_B \, g \, B_0}{h} \right) \cdot \left(\frac{3 \cos^2\theta - 1}{2} \right) - D_{ref} \tag{1}$$

where T is the temperature, θ is the angle of the NV bond axis relative to B_0, ν_{mw} is the readout microwave frequency, μ_B is the Bohr magneton, $g = 2.0028$ the g-factor for NV$^-$ [4], B_0 is the static magnetic field, h the Planck constant, and $D_{ref} = 2.87$ GHz [4].

Bond alignment with B_0 was established by mounting the sample on a sample holder with an angle of 35° to the laser beam and rotating the holder until one of the NV defect axes was parallel to the magnetic field, as determined by peak location in the observed EPR spectrum. Exact bond angles of all four defect orientations relative to the magnetic field were determined by modeling the spectra under different crystal orientations until the peak positions could be overlaid to those in the experimental spectra. This method has been used previously [31]. The angle between NV bond axis and external magnetic field in the following data is 5.0° (see 2, supplemental material).
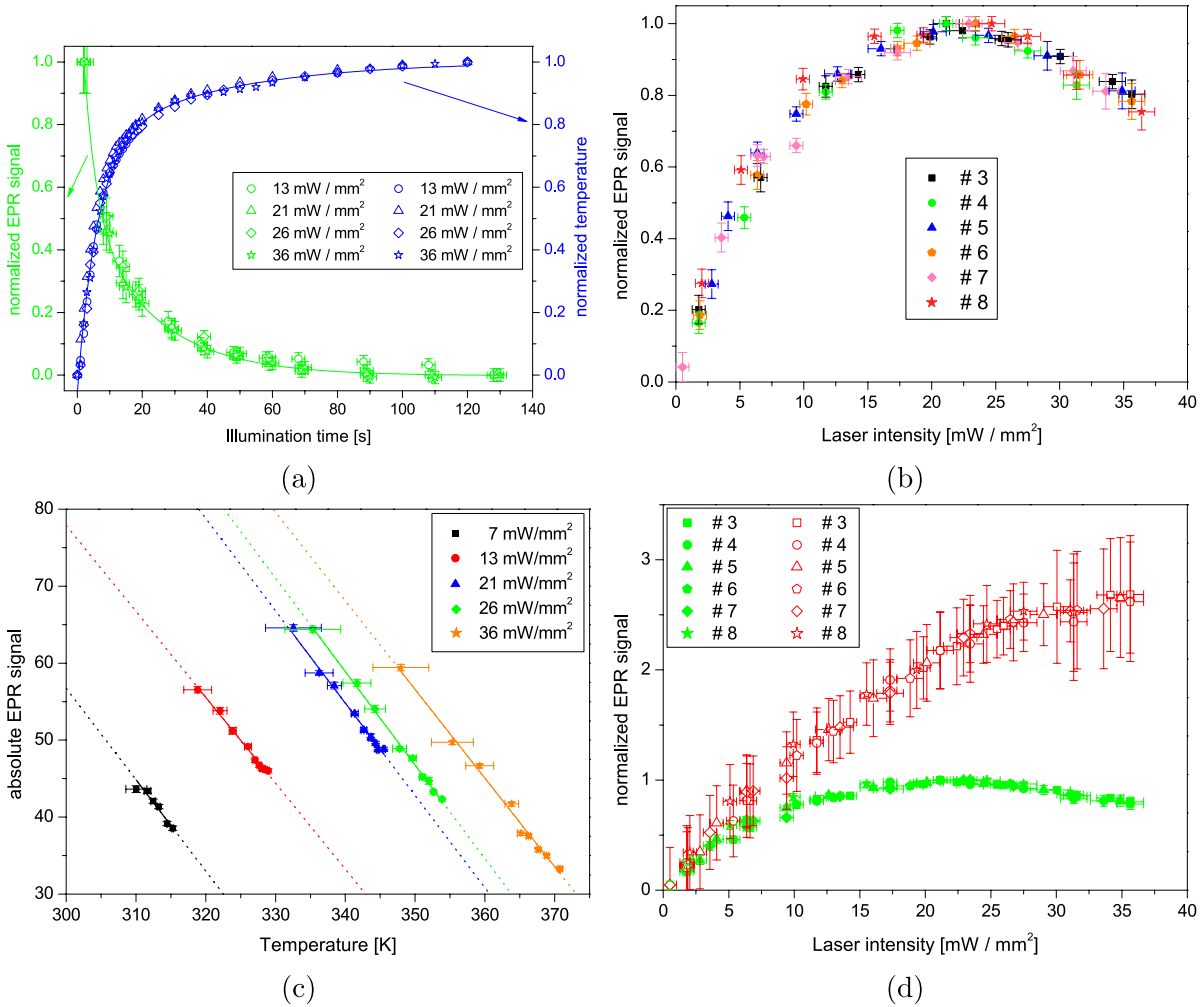
Figure 2. Peak-to-peak height of dispersive EPR spectrum for NV⁻-doped diamond samples. We analyzed spin state transitions from $|0\rangle$ to $|+1\rangle$ of laser-induced hyperpolarized NV⁻ defects. (a) Graphical depiction of correlation between temperature and EPR signal over the first 130 s of exposure. Normalization was carried out by setting the saturation temperature to 1 and the corresponding EPR signal to 0. Double exponential fits reveal equal time constants (see 5, supplemental material). Error bars indicate noise and uncertainty in illumination time. (b) Normalized EPR signal after 120 s of 532 nm laser light exposure for samples #3–#8. Laser intensities of 0.5–36 mW mm⁻² were applied. Error bars in laser intensities are fluctuations of laser power, and errors in EPR signals are the standard deviation of five measurements. (c) Absolute EPR signal of sample #5 at different temperatures and laser intensities. Domain of illumination time (8–120 s) was transformed into the temperature domain (310–372 K) through calibration (see 3, supplemental material). Lines are linear fits, extrapolations are displayed by dotted lines. Error bars in temperature are propagated through the domain transformation, in errors in EPR signal by spectral noise. (d) Green/filled: normalized measured EPR data from figure (a). Red/open: Derived EPR signal assuming temperature is held constant at 300 K under different laser intensities. A correction function was determined from the data in figure (c) (see 8, supplemental material). Error bars in laser intensity are fluctuations of laser power, and errors in EPR signal are propagated from standard deviations and uncertainty of the linear fits in figure (b).

We observe a change in $D_{\mathrm{obs}}(\mathrm{T}, \theta)$ of 10.6 GHz over the range of 308–397 K. This trend is consistent with recent work wherein the authors employed ODMR detection and heated the sample using conventional temperature adjustment methods [26, 28–30].

3.2. Laser-induced heating effects on NV⁻ hyperpolarization

We measured the EPR peak-to-peak height of optically hyperpolarized NV⁻ defects in samples #3–#8 at laser intensities up to 36 mW mm⁻². The EPR signal is proportional to the

population difference between spin states of the defect and therefore a gauge for hyperpolarization.

In time-resolved measurements, we observed a decreasing EPR signal with increasing illumination time over a timescale of 2 min. Time-resolved diamond temperature measurements show rising temperatures of up to 372 K within our apparatus at 36 mW mm⁻² laser intensity (see 3, supplemental material). The correlation of the two phenomena is depicted in figure 2(a). Normalization of the EPR signal, measured at 13–36 mW mm⁻², and the corresponding temperatures to values from 0 to 1 reveals equal double exponential time
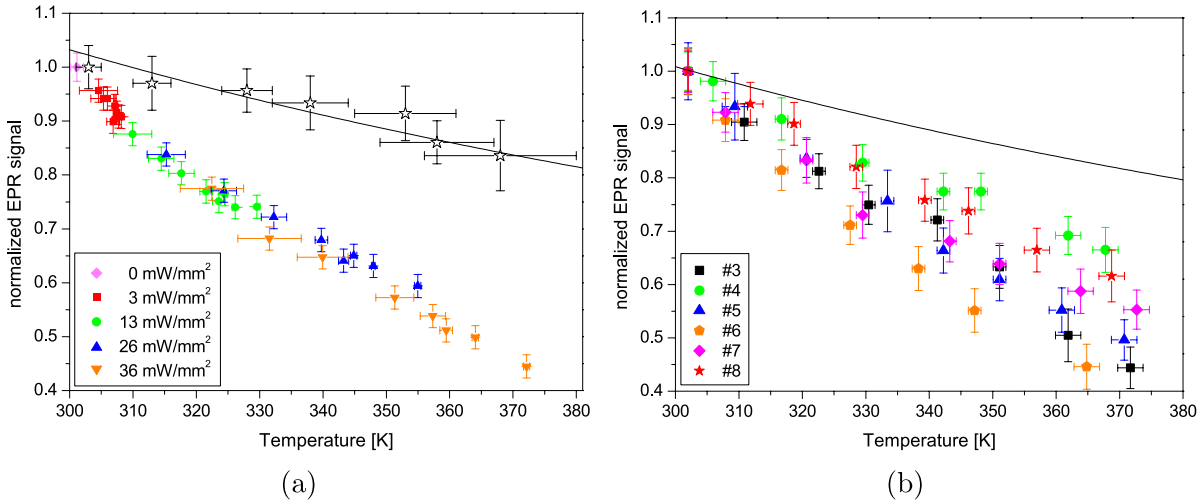
J. Phys. D: Appl. Phys. **50** (2017) 395307

C Szczuka *et al*

Figure 3. Peak-to-peak height of the normalized dispersive EPR spectrum for P1 center spin state transitions from $|-1/2\rangle$ to $|+1/2\rangle$. The black line shows the expected trend according to thermal equilibrium as given by the Boltzmann expression. Error bars in temperature are propagated through the domain transformation; errors in EPR signal derive from spectral signal-to-noise. (a) Filled: Normalized P1 EPR signal dependence of sample #3 on temperature rise evoked by laser-induced heating. Laser intensities from 0–36 mW mm^{-2} and illumination times of 3–120 s were used. Calibration of illumination time and temperature was conducted separately (see 3, supplemental material). Open stars: EPR signal of sample #3 in a previously heated oil bath within an EPR tube. Calibration of oil cooling time was conducted separately. (b) P1 EPR signal decline with temperature of samples #3–#8 after 120 s of laser exposure.

constants within the error (see 5, supplemental material). Photoionization occurs on the time scale of milliseconds [34–36] and polarization through intersystem crossing to an equilibrium state in the time scale of nanoseconds [3]. Further, we do not expect relaxation processes due to continuous laser exposure throughout the measurements. Thus, the observed time-dependent EPR signal decrease is exclusively due to temperature changes with time. Cooling experiments (see 6, supplemental material) reveal equal results.

In order to accurately compare the effects of differing laser intensities, measurements were performed after 120 s of illumination when steady state temperature had been reached (see 4, supplemental material). The data are displayed in figure 2(b). Here, normalization has been carried out by setting the maximum value of EPR signal to 1.0. Firstly, we show that optically enhanced polarization is independent of NV^{-} (P1) defect concentration in the range of 4.2–8.7 ppm (22–101 ppm). Previously, a dependence on NV^{-} concentration was postulated [31]; we attribute the discrepancy to the fact that temperature effects were not considered previously and that these differences in temperature led to variations in polarization between experiments. Secondly, the shape of the data curves imply an ideal laser intensity of approximately 22 mW mm^{-2} for maximum hyperpolarization. Similar behavior was observed recently with maxima at various laser intensities [25, 31, 32]. We expect sample temperature to have affected these previous findings.

To resolve EPR signal at different temperatures, we measured time-dependent EPR signal and calibrated illumination time and temperature (see 3, supplemental material). Plotting the absolute EPR signal as a function of temperature yields figure 2(c). Spectra were recorded from 8–120 s laser irradiation at laser intensities of 7–36 mW mm^{-2}. We show that for a given laser intensity the EPR signal decreases linearly with

temperature. The slope of -1.17 ± 0.04 K^{-1} is independent of laser intensity (see 7, supplemental material). Those data points with lowest EPR signal at each laser intensity form the bell shaped graph from figure 2(b), as laser intensity is proportional to the temperature after 120 s of exposure (see 4, supplemental material).

Figure 2(c) shows that at isothermal conditions the EPR signal differs vastly at various laser intensities. Deriving a function by taking the intercepts of the fit lines in figure 2(c) with an isotherm can be used to decouple the data in figure 2(b) from heating effects (see 8, supplemental material). In this way, we predict the polarization behavior if the diamond temperature could be held constant. The result is shown in figure 2(d). The green filled signs are transferred from figure 2(b). The red open signs represent the predicted EPR signal at a constant temperature of 300 K. In contrast to the previously anticipated ideal laser intensity, hyperpolarization is continuously rising. The large error in this prediction prevents assertions whether the EPR signal is linearly growing or saturating. However, if *in situ* cooling were possible NV^{-} polarization would continue to increase even at the highest laser intensities measured here.

3.3. Laser-induced heating effects on P1 polarization

We also investigated the effects of laser-induced heating on EPR signals emanating from P1 centers. The filled symbols in figure 3(a) show the experimental data for time-dependent measurements of sample #3 as a function of temperature at laser intensities from 0–36 mW mm^{-2}. As expected, the P1 EPR signal is monotonically decreasing. Independence of laser intensity is expected and observed in the strong overlap between different applied laser intensities.

J. Phys. D: Appl. Phys. **50** (2017) 395307

C Szczuka *et al*

Surprisingly, the decline in signal is greater than expected according to thermal equilibrium given by a Boltzmann factor. When externally heating the diamond with an oil bath, however, the temperature-dependence follows the expected Boltzmann trend (open stars and black line). Figure 3(b) shows that the EPR signal of all six samples studied here decreases more rapidly than expected in the presence of thermal laser-induced heating. To confirm the absence of unidentified laser effects on the microwave cavity, we measured EPR signal of Cr-(III) in a ruby with laser-induced heating, and it indeed followed the Boltzmann trend (see 9, supplemental material).

We preclude photoionization as the reason for this non-Boltzmann behavior because: (1), the decline in P1 signal is independent of laser intensity; (2), the timescale of seconds to minutes in our experiments is much greater than the millisecond timescale for photoionization [34–36] so it would not affect data at constant laser intensity; (3), the applied laser intensities are not expected to cause significant photoionization [37]; and (4), photoionization of NV^- would induce formation of P1 due to surplus of electrons, yielding an increase in EPR signal as opposed to the observed decrease [35]. A possible explanation for this athermal signal behavior is that the P1 centers are being polarized by hot electrons, combatting thermal polarization and lowering their EPR signal from the expected Boltzmann trend.

There is a rough correlation between the degree of deviation from the Boltzmann trend and the defect concentrations [33] in the diamonds. The diamonds with higher concentrations deviate more from the Boltzmann trend, with higher concentrations implying decreased average distances between all defects. The limited scope of samples with varying P1 and NV^- concentration prevents us from drawing definitive conclusions, and further work is needed to explore the concentration-dependence of this phenomenon.

4. Conclusion

We characterized laser-induced heating effects on NV^- and P1 defects in HPHT Type Ib diamonds. Illumination by a 532 nm laser with laser intensities up to 36 mW mm^{-2} results in sample heating up to 372 K in the limit of our experiment setup. Heating occurs exponentially and steady state is reached after approximately 120 s.

This heating is sufficient to observe NV^- zero-field splitting shifts as reported previously in non-optical heating experiments [26–30] and saturates NV^- polarization. By decoupling laser-induced heating from optical pumping effects, we predict the NV^- polarization to grow steadily with laser intensity at isothermal conditions.

Our findings affect design decisions of diamond-based polarization devices; cooling strategies to mitigate laser heating are crucial for maximizing polarization and stabilizing the zero-field splitting, especially if large laser intensities and/ or prolonged laser exposure are employed.

The P1 EPR signal is independent of laser intensity and decreases with temperature, yet does not follow the expected Boltzmann decline. We preclude photoionization and postulate that photoexcitation and subsequent capture at the P1 centers yields non-Boltzmann populations of the P1 eigenstates. Nevertheless, hyperpolarization of P1 centers offers improved polarization transfer schemes to nuclei and electrons outside of the diamond due to their higher abundance (given current sample preparation methods). Further work should seek to increase and control this athermal P1 signal.

Acknowledgments

References

[1] Doherty M W, Manson N B, Delaney P, Jelezko F, Wrachtrup J and Hollenberg L C L 2013 *Phys. Rep.* **528** 1–45
[2] Manson N B, Harrison J P and Sellars M J 2006 *Phys. Rev. B* **74** 104303
[3] Tetienne J P, Rondin L, Spinicelli P, Chipaux M, Debuisschert T, Roch J F and Jacques V 2012 *New J. Phys.* **14** 103033
[4] Loubser J H N and van Wyk J A 1978 *Rep. Prog. Phys.* **41** 1201–48
[5] Plakhotnik T and Gruber D 2010 *Phys. Chem. Chem. Phys.* **12** 9751–6
[6] Toyli D M, Christle D J, Alkauskas A, Buckley B B, Van de Walle C G and Awschalom D D 2012 *Phys. Rev.* X **2** 031001
[7] Balasubramanian G *et al* 2008 *Nature* **455** 648–51
[8] Taylor J M, Cappellaro P, Childress L, Jiang L, Budker D, Hemmer P R, Yacoby A, Walsworth R and Lukin M D 2008 *Nat. Phys.* **4** 810–6
[9] Dolde F *et al* 2011 *Nat. Phys.* **7** 459–63
[10] Dolde F, Doherty M W *et al* 2014 *Phys. Rev. Lett.* **112** 097603
[11] Kurtsiefer C, Mayer S, Zarda P and Weinfurter H 2000 *Phys. Rev. Lett.* **85** 290–3
[12] McGuinness L P *et al* 2011 *Nat. Nanotechnol.* **6** 358–63
[13] Gaebel T *et al* 2006 *Nat. Phys.* **2** 408–13
[14] Hanson R, Mendoza F M, Epstein R J and Awschalom D D 2006 *Phys. Rev. Lett.* **97** 087601
[15] Hebbache M 2011 *Phys. Rev. B* **84** 193204
[16] Smeltzer B, McIntyre J and Childress L 2009 *Phys. Rev. A* **80** 050302
[17] King J P, Coles P J and Reimer J A 2010 *Phys. Rev. B* **81** 073201
[18] Fischer R, Jarmola A, Kehayias P and Budker D 2013 *Phys. Rev. B* **87** 125207
[19] Pagliero D, Laraoui A, Henshaw J D and Meriles C A 2014 *Appl. Phys. Lett.* **105** 242402
[20] Álvarez G A, Bretschneider C O, Fischer R, London P, Kanda H, Onoda S, Isoya J, Gershoni D and Frydman L 2015 *Nat. Commun.* **6** 8456
[21] King J P, Jeong K, Vassiliou C C, Shin C S, Page R H, Avalos C E, Wang H J and Pines A 2015 *Nat. Commun.* **6** 8965
[22] Abrams D, Trusheim M E, Englund D, Shattuck M D and Meriles C A 2014 *Nano Lett.* **5** 2471–78
[23] Doherty M W *et al* 2014 *Phys. Rev. Lett.* **112** 047601

J. Phys. D: Appl. Phys. **50** (2017) 395307

C Szczuka *et al*

[24] Ivády V, Simon T, Maze J R, Abrikosov I A and Gali A 2014 *Phys. Rev. B* **90** 235205

[25] Bourgeois E, Jarmola A, Siyushev P, Gulka M, Hruby J, Jelezko F, Budker D and Nesladek M 2015 *Nat. Commun.* **6** 8577

[26] Acosta V M, Bauch E, Ledbetter M P, Waxman A, Bouchard L S and Budker D 2010 *Phys. Rev. Lett.* **104** 070801

[27] Acosta V M, Bauch E, Jarmola A, Zipp L J, Ledbetter M P and Budker D 2010 *Appl. Phys. Lett.* **97** 174104

[28] Chen X D, Dong C H, Sun F W, Zou C L, Cui J M, Han Z F and Guo G C 2011 *Appl. Phys. Lett.* **99** 161903

[29] Doherty M W, Acosta V M, Jarmola A, Barson M S J, Manson N B, Budker D and Hollenberg L C L 2014 *Phys. Rev. B* **90** 041201

[30] Plakhotnik T, Doherty M W, Cole J H, Chapman R and Manson N B 2014 *Nano Lett.* **14** 4989–96

[31] Drake M, Scott E and Reimer J A 2016 *New J. Phys.* **18** 013011

[32] Loretz M, Takahashi H, Segawa T F, Boss J M and Degen C L 2017 *Phys. Rev. B* **95** 064413

[33] Scott E, Drake M and Reimer J A 2016 *J. Magn. Reson.* **264** 154–62

[34] Manson N B and Harrison J P 2005 *Diam. Relat. Mater.* **14** 1705–10

[35] Gaebel T *et al* 2006 *Appl. Phys. B* **82** 243–6

[36] Aslam N, Waldherr G, Neumann P, Jelezko F and Wrachtrup J 2013 *New J. Phys.* **15** 013064

[37] Lawson S C, Fisher D, Hunt D C and Newton M E 1998 *J. Phys.: Condens. Matter* **10** 6171–80